



J. Serb. Chem. Soc. 75 (11) 1595–1604 (2010)
JSCS–4079

Crystal growth of $K_2TiGe_3O_9$ in the glass

SNEŽANA R. GRUJIĆ^{1*#}, NIKOLA S. BLAGOJEVIĆ^{1#}, MIHAJLO B. TOŠIĆ^{2#},
VLADIMIR D. ŽIVANOVIĆ² and ZAGORKA S. AČIMOVIĆ-PAVLOVIĆ¹

¹Faculty of Technology and Metallurgy, 4 Karnegijeva St., 11000 Belgrade and ²Institute for
Technology of Nuclear and other Mineral Raw Materials, Franchet d'Esperey 86,
11000 Belgrade, Serbia

(Received 18 November 2009, revised 29 July 2010)

Abstract: The kinetics and mechanism of isothermal crystal growth of $K_2TiGe_3O_9$ from a glass of the same stoichiometric composition were studied. The crystal growth rate, U , in the range 1×10^{-11} – 1.27×10^{-10} m s⁻¹ was experimentally determined in the temperature interval 540–600 °C. In the range of high undercooling, Δt , 435–375 °C, spherical crystals growing at (374 ± 19) kJ mol⁻¹ was observed.

Keywords: crystal growth; $K_2TiGe_3O_9$; kinetics; mechanism; glass.

INTRODUCTION

Binary alkali germanates exhibit a characteristic behavior known as the “germanate anomaly effect”.^{1–3} This behavior means the presence of extremes on the curves showing the dependence of some properties (density, refractive index, glass transition temperature and viscosity) on the content of the alkali oxide. Studies of the behaviors of ternary germanate glasses are not very numerous. Recent investigations^{4–6} showed that during crystallization of some K_2O – TiO_2 – GeO_2 glasses with a high content of TiO_2 , crystals of $K_2TiGe_3O_9$ were formed. The presence of these crystals enables non-linear optical materials showing second harmonic generation to be obtained.⁶ Such materials have great potential for different applications. Due to this, the phase formation of $K_2TiGe_3O_9$ has been a subject of reinforced interest because knowledge of crystal nucleation and growth processes of $K_2TiGe_3O_9$ is important for the preparation of crystallized glasses possessing the desired microstructure and properties.

The results of a study of $K_2TiGe_3O_9$ crystal nucleation in a $K_2O \cdot TiO_2 \cdot 3GeO_2$ undercooled melt were previously published.⁷ In the present study, attention was

* Corresponding author. E-mail: grujic@tmf.bg.ac.rs

Serbian Chemical Society member.

doi: 10.2298/JSC091118120G

focused on the kinetics and mechanism of crystal growth of $\text{K}_2\text{TiGe}_3\text{O}_9$ from its undercooled melt.

EXPERIMENTAL

The $\text{K}_2\text{O}\cdot\text{TiO}_2\cdot 3\text{GeO}_2$ glass was prepared by melting a homogeneous mixture of reagent grade K_2CO_3 , TiO_2 (both Fluka Chemica,) and GeO_2 (electronic grade) in a platinum crucible. The melting was performed in an electric furnace, Carbolite BLF 17/3, at $t = 1300^\circ\text{C}$ during $\tau = 2$ h. The glass was obtained by quenching the melt on a steel plate. Powder X-ray diffraction analysis (XRD) confirmed the quenched melts to be vitreous. The glass samples were transparent, without visible residual gas bubbles.

The experiments were performed under isothermal conditions with bulk samples in a one-stage regime in an electric furnace, Carbolite CWF 13/13, with automatic regulation and a temperature accuracy of $\pm 1^\circ\text{C}$. The glass samples were heated at a heating rate $\beta = 10^\circ\text{C min}^{-1}$ up to the desired temperature of heat treatment and maintained at the chosen temperature for different times. The heat treatment temperatures, t_c , were in the range $540\text{--}600^\circ\text{C}$. The samples were maintained at the selected temperature for times, τ_c , in the range $10\text{--}1000$ min. Finally, the samples were removed from the furnace and crushed in an agate mortar for X-ray and SEM analyses.

A Jeol JSM 6460 microscope was used for the scanning electronic microscopy (SEM) investigations. The samples for SEM investigation were gold sputtered. The diameters of circular intersections of the particles were determined from the SEM micrographs. The crystal growth rate, U , at the treatment temperature, t , was determined from the time dependence of the largest circular cross-section diameter, d .

The XRD method was used to determine the phase composition. The XRD patterns were obtained on a Philips PW-1710 automated diffractometer using a Cu tube operated at 40 kV and 32 mA. The instrument was equipped with a diffracted beam curved graphite monochromator and a Xe-filled proportional counter. The diffraction data were collected in the 2θ Bragg angle range from 4 to 70° , counting for 0.25 s at every 0.02° step. The divergence and receiving slits were fixed 1 and 0.1, respectively. The XRD measurements were performed at room temperature in a stationary sample holder.

RESULTS AND DISCUSSION

The results of the chemical analysis show that a glass composition: $19.27\text{K}_2\text{O}\cdot 16.8\text{TiO}_2\cdot 63.93\text{GeO}_2$ (wt. %) was obtained. This composition is close to the stoichiometric one $\text{K}_2\text{O}\cdot\text{TiO}_2\cdot 3\text{GeO}_2$.

The XRD patterns of samples thermally treated under different conditions are shown in Fig. 1, from which it can be seen that $\text{K}_2\text{TiGe}_3\text{O}_9$ was the only phase formed during the crystallization of this glass, *i.e.*, polymorphic crystallization occurred.⁸

The SEM micrographs of these samples are presented in Fig. 2. It is obvious that the nucleation process commenced within the bulk of the melt and that the morphology of the growing crystals was spherical.

A previous investigation of the nucleation of this glass showed that the temperature ranges of nucleation and crystal growth partly overlapped.⁷ Accordingly, isothermal, single-stage heat treatment experiments were performed. The

largest circular cross-section diameters, d , measured as a function of time at 540, 560, 580, 590 and 600 °C are shown in Figs. 3a–3d. The crystal growth rates were obtained from the slope of the lines.

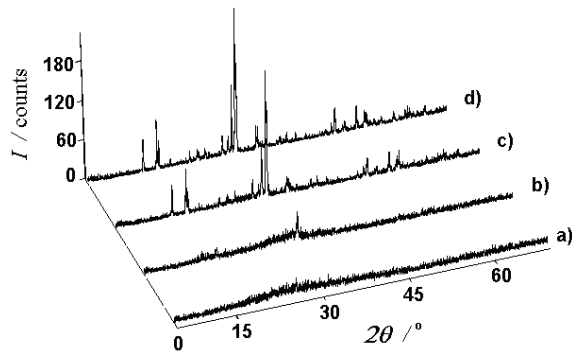
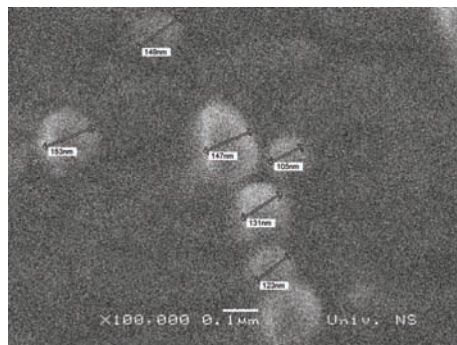
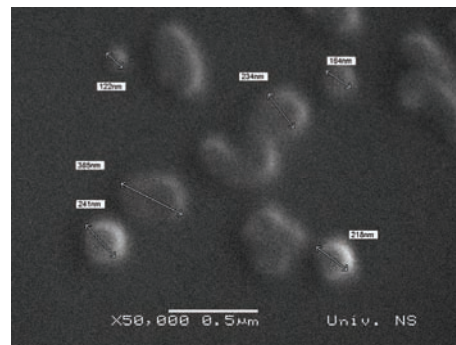


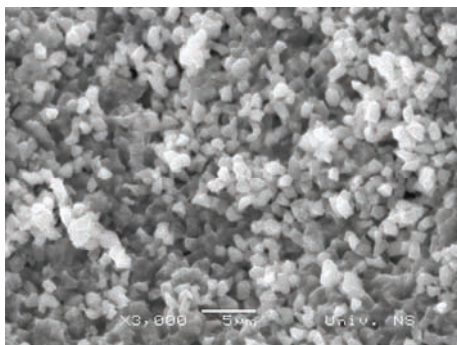
Fig. 1. XRD Patterns of: a) glass, b) sample crystallized at $t = 580$ °C for $\tau = 38$ min, c) sample crystallized at $t = 590$ °C for $\tau = 30$ min and d) sample crystallized at $t = 640$ °C for $\tau = 1000$ min.



(a)



(b)



(c)

Fig. 2. SEM Micrographs of crystallized samples after heat treatment at: a) $t = 580$ °C for $\tau = 38$ min, b) $t = 590$ °C for $\tau = 30$ min and c) $t = 640$ °C for $\tau = 1000$ min.

The experimentally determined crystal growth rate and nucleation rate as a function of temperature are presented in Fig. 4.

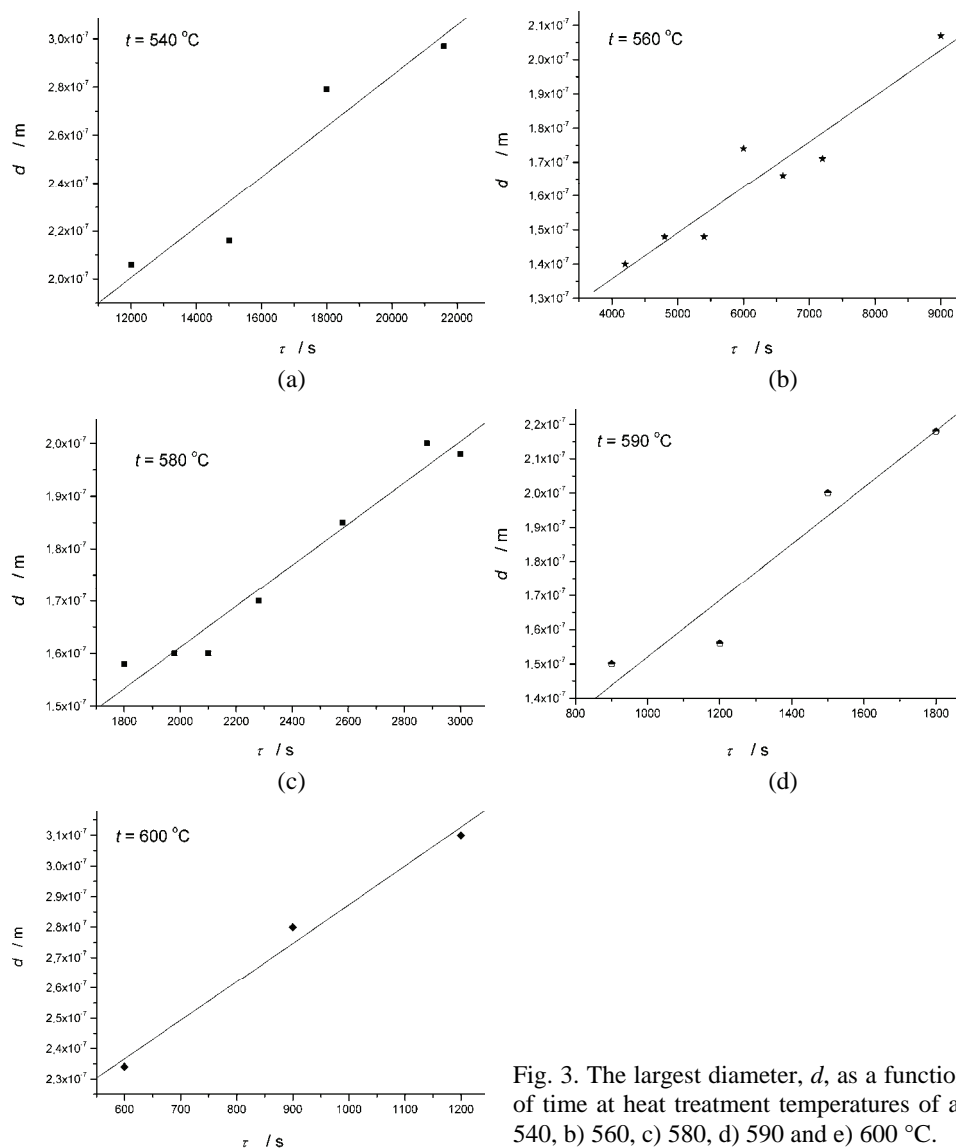


Fig. 3. The largest diameter, d , as a function of time at heat treatment temperatures of a) 540, b) 560, c) 580, d) 590 and e) 600 $^{\circ}\text{C}$.

The kinetics and morphology of crystals growing from the melt are determined by the following factors: a) interface kinetics – the movement of material across the interface and its attachment to the crystal surface; b) material transfer – the diffusion of material in melt; c) heat transfer – the removal of latent heat of crystallization from the growing crystal surface and c) reconstructive transformation – the arrangement of atoms or ions species at the solid–liquid interface.⁹ Crystal growth from the melt is realized by different mechanisms. The condition

of the surface of a growing crystal and the degree of undercooling of the melt play decisive roles on the action of certain growth mechanisms. Three standard models are employed to describe crystal growth and to predict the kinetic behavior and morphology: normal growth, screw dislocation growth and surface nucleation growth.^{10–13} An appropriate method for the estimation of the surface condition of a growing crystal (crystal–liquid interface) and for the prediction of the growth mechanism is the Jackson criterion.¹³ Accordingly, for materials with small entropies of fusion $\Delta S_m < 2R$, the solid–liquid interface should be rough on an atomic scale. If the interface is atomically rough, continuous growth with non-faceted interface morphology occurs and the anisotropy of the growth rate is small, hence normal growth is expected. In contrast, for materials with large entropies of fusion $\Delta S_m > 4R$, the solid–liquid interface should be smooth. If the interface is atomically smooth, layer growth with faceted interface morphology occurs, either by a screw dislocation or a surface nucleation growth mechanism. Previous experimental studies showed that for numerous organic and inorganic glasses, screw dislocation growth is operative. For glasses, crystallization with normal growth is less characteristic while surface nucleation growth is not usual.¹⁰

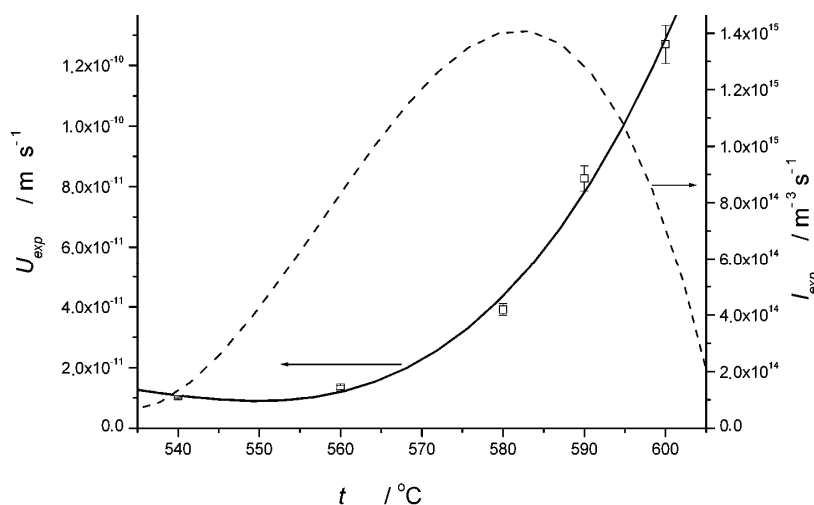


Fig. 4. U_{exp} and I_{exp} ⁷ in the temperature range 540–600 °C.

When the melt and crystal have the same chemical composition, for the case of growth at step sites provided by a screw dislocation intersecting the interface, the growth rate may be expressed by the relation:¹³

$$U = f\lambda v \left[1 - \exp\left(-\frac{\Delta G}{RT}\right) \right] \quad (1)$$

where U is the growth rate per unit area of the interface, f is the fraction of preferred growth sites on the interface and v is a frequency factor for transport at the interface, λ is the jump distance (of the order of atomic/molecular dimensions), ΔG is the free energy of crystallization (free energy difference in the transformation liquid-crystal, *i.e.*, the thermodynamic driving force for crystallization), T , is the temperature in Kelvin and R is the gas constant. The factor f is proportional to the undercooling $\Delta T = T_m - T$ according to the expression:

$$f = \frac{\lambda \Delta H_m \Delta T}{4\pi\sigma V_m T_m} \quad (2)$$

where T_m is the melting temperature, V_m is the molar volume of the crystalline phase, σ is the crystal/liquid interfacial and ΔH_m is the enthalpy of melting per mole. The frequency factor for transport at the interface, v , may be expressed as:

$$v = v_0 \exp\left(-\frac{\Delta G_D}{RT}\right) \quad (3)$$

where v_0 is the vibration frequency of the growth controlling atoms, ΔG_D is the activation free energy for diffusion across the interface (the activation energy of crystal growth).

Under the assumption that the molecular mobility necessary for crystal growth is similar to the transport of molecules in the bulk melt, then the activation energy for diffusion across the interface, ΔG_D , is equal to the activation energy for viscous flow, ΔG_η ($\Delta G_D \approx \Delta G$). Considering viscosity as an activated process, then it can be approximated by an equation of the form:¹⁴

$$\eta = \eta_0 \exp\left(\frac{\Delta G_\eta(T)}{RT}\right) \quad (4)$$

$$\eta_0 = \frac{kT}{l^3} \tau_0 \quad (5)$$

where l is the metal–oxygen bond length (Ge–O), τ_0 is a time of the order of the period of atomic vibration ($\tau_0 \approx 1/v_0$) and k is the Boltzmann constant.

By substitution of Eq. (5) into Eq. (4) and then into Eq. (3), the following expression is obtained:

$$v = \frac{kT}{l^3 \eta} \quad (6)$$

Introducing Eqs. (2) and (6) into Eq. (1), Eq. (7) is obtained:

$$U = \frac{\lambda^2 \Delta H_m k T \Delta T}{4\pi\sigma V_m l^3 T_m} \frac{1}{\eta} \left[1 - \exp\left(-\frac{\Delta G}{RT}\right) \right] \quad (7)$$

Using Eq. (7) and the values of the parameters given in Table I, the theoretical rate of $K_2TiGe_3O_9$ crystal growth can be calculated.

TABLE I. The parameters of $K_2TiGe_3O_9$ used for the estimation of U_{calc}

$k / J K^{-1}$ (Ref. 13)	1.3807×10^{-23}
λ / m (Ref. 15)	5.6×10^{-10}
l / m (Ref. 15)	1.77×10^{-10}
$V_m / m^3 mol^{-1}$ (Ref. 8)	123.6×10^{-6}
$\sigma / J m^{-2}$ (Ref. 8)	0.17
$\Delta G / J mol^{-1}$ (Ref. 7)	$\Delta G(T) = -102.97(1308.16 - T) + 108.27[(1308.16 - T) - T(\ln(1308.16/T))]$, T in K
$\eta / Pa s$ (Ref. 5)	$\eta = -0.286 + 1739/(T - 684)$, T in K

To obtain a more exact insight into the relation between the theoretical and experimental values of the growth rate of $K_2TiGe_3O_9$ crystals, this relation in a narrow temperature range 540–600 °C is presented in Fig. 5, from which it may be seen that a good agreement between the theoretical and experimental values of the growth rate of $K_2TiGe_3O_9$ crystals exists in the temperature interval 540–600 °C. This enables the crystal growth mechanism and the activation energy of crystal growth to be determined based on experimental values.

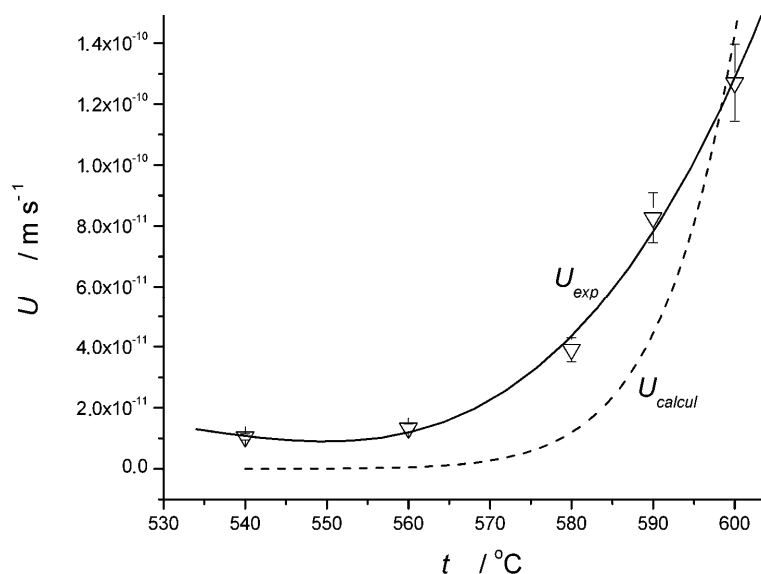


Fig. 5. Experimental (∇) and calculated (---) crystal growth rates according to Eq. (7) vs. t in the range 540–600 °C.

If in Eq. (1) the exponential factor expands in the series:

$$\exp \frac{\Delta G}{RT} = 1 - \frac{\Delta G}{RT} + \frac{1}{2!} \left(\frac{\Delta G}{RT} \right)^2 - \frac{1}{3!} \left(\frac{\Delta G}{RT} \right)^3 + \dots \quad (8)$$

and as significant, the first two terms in the series are taken into consideration, the following replacement can be made

$$\left[1 - \exp \left(-\frac{\Delta G}{RT} \right) \right] = \frac{\Delta G}{RT} = \frac{\Delta H_m (T_m - T)}{RT T_m} = \frac{\Delta H_m \Delta T}{RT T_m} \quad (9)$$

Replacement of Eq. (2), (3), (9) and $v_0 = kT/h$, $k = R/N_A$ (where h is the Planck constant and N_A is the Avogadro constant) in Eq. (1) gives:

$$U = \frac{\lambda^2 \Delta H_m^2}{4\pi\sigma V_m h N_A T_m^2} (\Delta T)^2 \exp \left(-\frac{\Delta G_D}{RT} \right) \quad (10)$$

The first term of the right side in Eq. (10) is independent of temperature, hence Eq. (10) may be written as:

$$U = K_1 (\Delta T)^2 \exp \left(-\frac{\Delta G_D}{RT} \right) \quad (11)$$

where $K_1 = \lambda^2 \Delta H_m^2 / (4\pi\sigma V_m h N_A T_m^2)$.

Using the experimental data of the crystal growth rate at temperatures in the interval 540–600 °C according to Eq. (11), the relation $\ln[U_{\text{exp}}/(\Delta T)^2]$ vs. $1/T$ shown in Fig. 6 was obtained. As can be seen in Fig. 6, the relationship can be described by a straight line of negative slope. This suggests that growth of

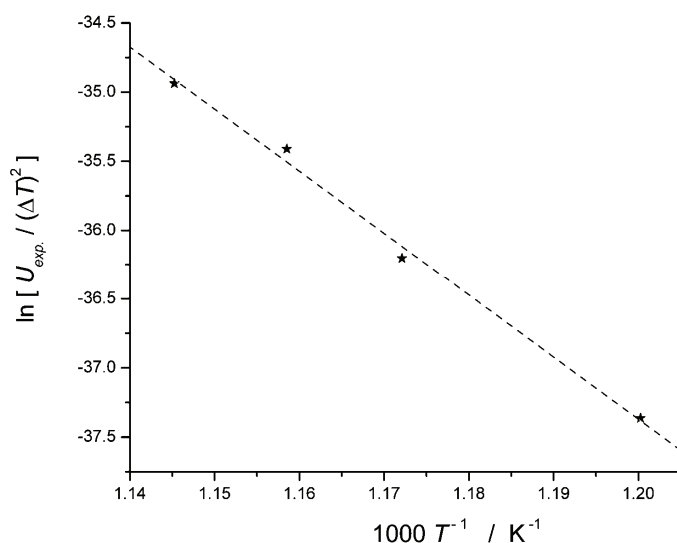


Fig. 6. Plot of $\ln[U_{\text{exp}}/(\Delta T)^2]$ vs. $1/T$.

$K_2TiGe_3O_9$ crystals occurs by the screw dislocation mechanism in the region of undercooling, Δt , 435–475 °C. From the slope of this line, the activation energy of crystal growth $\Delta G_D = (374 \pm 19)$ kJ mol⁻¹ was calculated.

In the range of large undercooling, the temperature dependence of the crystal growth rate substantially follows that of the viscosity of the liquid which crystallizes polymorphic and where crystal growth occurs by the screw dislocation growth mechanism. For comparison, the activation energy of viscous flow, $\Delta G_\eta(T)$, was calculated. Since $\Delta G_\eta(T)$ is temperature-dependent, the temperature range was selected in which the isothermal experiments were performed. The calculation was realized using data from Table I and Eq. (4). A value of $\Delta G_{\eta,560-600} = (372 \pm 12)$ kJ mol⁻¹ was obtained, which is in good agreement with ΔG_D .

CONCLUSIONS

The crystal growth kinetics of $K_2TiGe_3O_9$ from its melt under isothermal conditions was studied. The experiments were performed in the temperature range 540–600 °C. The crystal growth rates determined by SEM were in the range from 1×10^{-11} to 1.27×10^{-10} m s⁻¹. In this temperature range, the agreement between the theoretical and experimental values of the crystal growth rate of $K_2TiGe_3O_9$ is good. The analysis showed that in the region of high undercooling, Δt , 435–475 °C, the crystals of $K_2TiGe_3O_9$ grew by the screw dislocation mechanism. The activation energy of crystal growth $\Delta G_D = (374 \pm 19)$ kJ mol⁻¹ was calculated. This value corresponds to the activation energy of viscous flow in this temperature range.

Acknowledgment. The authors are grateful to the Ministry of Science and Technological Development of the Republic of the Serbia for financial support (Project No. 142041).

ИЗВОД

РАСТ КРИСТАЛА $K_2TiGe_3O_9$ У СТАКЛУ

СНЕЖАНА Р ГРУЉИЋ¹, НИКОЛА С БЛАГОЈЕВИЋ¹, МИХАЈЛО Б ТОШИЋ², ВЛАДИМИР Д ЖИВАНОВИЋ²
и ЗАГОРКА С АЋИМОВИЋ-ПАВЛОВИЋ¹

¹Технолошко-металуршки факултет, Карнегијева 4, 11000 Београд и ²Институт за технологију нуклеарних и других минералних сировина, Франше д'Ейереа 86, 11000 Београд

Под изотермским условима проучавана је кинетика и механизам раста $K_2TiGe_3O_9$ кристала из стакла истог стехиометријског састава. У интервалу температуре 540–600 °C експериментално су одређене брзине раста кристала, U , 1×10^{-11} – 1.27×10^{-10} m s⁻¹. Показано је да се у области високих потхлађења, Δt , 435–375 °C, раст сферних кристала ове фазе одвија по механизму завојне дислокације. Добијена је енергија активације раста кристала $\Delta G_D = (374 \pm 19)$ kJ mol⁻¹.

(Примљено 18. новембра 2009, ревидирано 29. јула 2010)

REFERENCES

1. M. K. Murthy, E. M. Kirby, *Phys. Chem. Glasses* **5** (1964)144

2. J. E. Shelby, *J. Am. Ceram. Soc.* **57** (1974) 436
3. E. F. Riebling, *J. Chem. Phys.* **39** (1963) 1889
4. S. R. Grujić, N. S. Blagojević, M. B. Tošić, V. D. Živanović, *Ceram. Silik.* **49** (2005) 278
5. S. Grujić, N. Blagojević, M. Tošić, V. Živanović, B. Božović, *J. Therm. Anal. Calor.* **83** (2006) 463
6. T. Fukushima, Y. Benino, T. Fujiwara, V. Dimitrov, T. Komatsu, *J. Solid State Chem.* **179** (2006) 3949
7. S. R. Grujić, N. S. Blagojević, M. B. Tošić, V. D. Živanović, J. D. Nikolić, *Ceram. Silik.* **53** (2009) 128.
8. Joint Committee on Powder Diffraction Standards (JCPDS), *Powder Diffraction File*, Card No. 27-0394, 1975
9. V. J. Fratello, J. F. Hays, F. Spaepen, D. Turnbull, *J. Appl. Phys.* **51** (1980) 6160
10. D. R. Uhlmann, in *Advances in Ceramics*, J. H. Simmons, D. R. Uhlmann, D. H. Beal, Eds., American Ceramic Society, Westerville, OH, 1982, p. 80
11. V. M. Fokin, M. L. F. Nascimento, E. D. Zanotto, *J. Non-Cryst. Solids* **351** (2005) 789
12. N. Diaz-Mora, E. D. Zanotto, V. M. Fokin, *Phys. Chem. Glasses* **39** (1998) 91
13. W. D. Kingery, H. K. Bowen, D. R. Uhlmann, *Introduction to Ceramics*, Wiley Interscience, New York, 1976, p. 340
14. I. Gutzow, J. Schmelzer, *The Vitreous State*, Springer, Berlin, 1995, p. 169
15. G. S. Henderson, H. M. Wang, *Eur. J. Mineral.* **14** (2002) 733.